On the formation of ultra-fine grained Fe-base alloys via phase transformations

Chezan, AR; Craus, CB; Chechenin, NG; Vystavel, T; Niesen, L; De Hosson, JTM; Boerma, DO

Published in:
Materials science and engineering a-Structural materials properties microstructure and processing

DOI:
10.1016/j.msea.2003.10.256

Publication date:
2004

Materials Science and Engineering A 367 (2004) 176–184

MATERIALS SCIENCE & ENGINEERING A

www.elsevier.com/locate/msea

On the formation of ultra-fine grained Fe-base alloys via phase transformations

A.R. Chezan*, C.B. Craus, N.G. Chechenin, T. Vystavel, L. Niesen, J.Th.M. De Hosson, D.O. Boerma

Departments of Nuclear Solid State Physics and Applied Physics, Materials Science Center and the Netherlands Institute for Metals Research, University of Groningen, Nijenborgh 4, 9747 AG Groningen, The Netherlands

Received 17 March 2003; received in revised form 29 September 2003

Abstract

This paper concentrates on the formation of ultra-fine grained Fe-base alloys via phase transformations. In particular the manipulation of the microstructure of Fe–Ni–Ti and Fe–Ni–Cr alloys via phase cycling in the Fe–N system was investigated. Transitions between bcc (α-Fe), fcc (γ′-Fe_4N) and hcp (ε-Fe_xN) structures were obtained by gaseous nitriding of cold-rolled foils. During cycling the rate of transformation was progressively retarded due to recovery as a result of the nitriding/reduction treatment. The α ↔ γ′ cycling at 380 °C did not produce significant grain reorientation in neither Fe–Ni–Ti nor Fe–Ni–Cr alloys. After α ↔ ε cycling at 400 °C the texture of the Fe–Ni–Ti alloy was preserved. Reduction of texture in this alloy was obtained at 500 °C. Grain refinement and grain reorientation took place after α ↔ ε transformations in FeNiCr alloy at 400 °C. An optimum of five cycles was found for structure refinement to about 100 nm. Increasing the number of cycles leads to further coarsening of the microstructure.

Keywords: Grain refining; Phase transformations; Iron alloys; Microscopy; X-ray diffraction

1. Introduction

Several physical properties of materials are strongly affected by the grain size. For instance, in metallic systems the yield stress decreases with increasing grain size over a considerable range as described by the well-known Hall–Petch equation [1]. The grain boundaries may act as obstacles for moving dislocations, leading to a pile-up of dislocations in front of the boundary. An analogous effect is the "strengthening" of a ferromagnetic material, i.e. the increase of the coercive field with decreasing grain size in the micrometer to the tens of nanometer range. This reflects the reduction of the mobility of the magnetic domain walls by the interaction with the grain boundaries.

When the dimensions of the grains become comparable with the characteristic length of the physical phenomenon involved, conventional scaling laws often break down and may even reverse [2]. An example is Cu, where the upper limit of the classical Hall–Petch behavior is reported to be 50 nm [3]. The latter is determined by the line tension of a lattice dislocation. In magnetism, a strong drop in the coercivity is obtained when the grain size becomes smaller than the exchange correlation length, e.g. 35 nm in Fe. This latter effect has led to the discovery of a new class of ultra-soft magnetic materials [4]. These findings strongly suggest that both functional and mechanical properties can be tailored by controlling the grain size of the material.

Two different routes can lead to materials with grain sizes in the 1–100 nm range: devitrification of amorphous phases or refinement of the structure of materials with micrometer-sized grains. The main drawback of devitrification of amorphous films or ribbons is the fact that the quantity of materials obtained in the amorphous phase is relatively small. In contrast, for bulk materials, usually with a grain size in the micrometer-millimeter range, grain refinement can be obtained by thermomechanical procedures. By cold rolling and recrystallization materials with grain size of the order of 1 μm have been obtained [5]. In this method the relatively high temperature required for recrystallization hampers a further decrease of the average grain size below the micrometer range.

* Corresponding author. Tel.: +31-50-3634901; fax: +31-50-3634881.
E-mail address: chezan@phys.rug.nl (A.R. Chezan).

0921-5093/$ – see front matter © 2003 Elsevier B.V. All rights reserved.
doi:10.1016/j.msea.2003.10.256

Reduction of the size of the grains to the nanometer range can be obtained by modification of the microstructure via phase transitions at low temperatures. For example, for fcc austenitic alloys (32Ni, 26Ni–Cr–Ti) with the temperature of the martensitic transformation below room temperature, grain sizes of the order of 10–80 nm have been obtained during forward and reverse martensitic $\gamma \rightarrow \alpha^1 \rightarrow \gamma$ transformations [6].

For bcc materials (Fe-based alloys) a possibility to keep the transformation temperature at relatively low values is to employ thermo-chemical nitriding in an NH_3/H_2-gaseous mixture followed by denitriding in a H_2 atmosphere. By a nitriding treatment, transitions between bcc and fcc or hcp structures can be obtained at temperatures as low as 300 °C. It should be noted that in order to have an efficient averaging out of the magnetocrystalline anisotropy or effective obstacles for dislocation movement, the reduction of the grain size must involve also significant change in misorientation between the grains. The new smaller grains which are formed must be randomly oriented.

In previous studies by the authors [7] it was shown that the transitions between bcc, fcc and hcp crystal structures occur at 300 °C during nitriding of a thin epitaxial Fe layer. As the nitrogen content in the film increases, the sequence of various phases is: α-Fe (bcc) → α′-Fe_8N, α″-$Fe_{16}N_2$ (bct) → γ′-Fe_4N (fcc) → ε-Fe_xN ($2 \leq x \leq 4$) (hcp). The bcc → fcc transition takes place via a bct intermediate phase. The {1 0 0} planes between the bcc and bct structures stay parallel and the tetragonal *c* axis is perpendicular to the plane of the layer; in other words the lattice of a thin layer expands perpendicular to the substrate as the nitrogen content increases. The bct → fcc transformation is governed by a Pitch-type OR (orientation relationship) expressed as: $[0\,\bar{1}\,1]_{\gamma'} \| [\bar{1}\,1\,1]_{\alpha'}$ and $(0\,1\,1)_{\gamma'} \| (1\,\bar{1}\,2)_{\alpha'}$. This is equivalent to a rotation of 45° around the [0 0 1] direction and a slight tilt (6.2°) of the (1 0 0) planes of the γ′-phase around the [1 1 0] direction. If we neglect, to a first approximation, the 6.2° rotation, the bcc → fcc transformation is then governed by a Bain OR expressed by $[\bar{1}\,1\,0]_{fcc} \parallel [1\,0\,0]_{bcc}$ and $(0\,0\,1)_{fcc} \| (0\,0\,1)_{bcc}$. For a material having a (1 0 0) texture, one ⟨1 0 0⟩ direction is perpendicular to the plane of the sample and two are in the plane of the sample. Correspondingly, the γ′-phase can be formed as a result of a rotation around an axis perpendicular to, or in the plane of the film. In the following such possibilities to realize a phase transition will be called "channels". Depending on the orientation of the rotation axis with respect to the plane of the film the fcc phase can grow with the (1 0 0) or (1 1 0) planes parallel to the surface. In the back transformation (fcc → bcc) the new bcc structure can have (1 0 0), (1 1 0) or (2 2 1) planes parallel to the surface. To create new crystal orientations during cycling, the channel in the forward and backward reaction should be different. Due to the misfit between the α-, α′- and γ′-phases, strain will build up in the material during phase transformation. If this strain does not affect the channel for the transformation and all the possible ORs occur with about equal probabilities, grain refinement and grain reorientation can be obtained by repeated cycling of bcc → fcc transitions [7]. When the nitrogen concentration in the film increases further, the hcp structured ε-Fe_xN phase is formed. If no significant diffusion of the lattice atoms takes place, the fcc → hcp transition is governed by an OR expressed by: $[0\,1\,0]_{hcp} \| [1\,\bar{1}\,0]_{fcc}$ and $(0\,0\,1)_{hcp} \| (1\,1\,1)_{fcc}$. Then, in a reversible transformation of bcc → hcp (via fcc), the large choice of the relative orientations of the "habit" planes leads to a stronger grain refinement and grain reorientation as compared to the bcc ↔ fcc case. It should be also noted that nitriding epitaxial Fe layers leads to the formation of textured γ′- and ε-phases. Due to the presence of the substrate the stress release during phase transformations in thin films takes place perpendicular to the plane of the layer leading to the formation of textured phases.

In this paper, we report on the manipulation of the microstructure of $Fe_{94}Ni_4Ti_2$ and $Fe_{93}Ni_4Cr_3$ alloys via phase transformations in the Fe–N system. In these systems TiN and CrN precipitates respectively are formed during nitriding. The influence of these precipitates on the phase transformation is discussed. It will be shown that, under certain treatment conditions, cyclic phase transformation leads to a progressive multiplication of the number of different grain orientations and causes further grain refinement.

2. Experimental procedures

Fe + Ni (4 at.%) + Ti (2 at.%) and Fe + Ni (4 at.%) + Cr (3 at.%) alloys were produced by melting the constituents of high purity in an induction furnace with cold walls. Slices (0.5 mm thick) of bulk materials were cold-rolled in two perpendicular directions to 2–4 μm thick foils (≈99% reduction of the initial thickness). The foils were nitrided at a temperature within the range of 300 °C to 500 °C in a convection furnace [8] in an $NH_3 + H_2$ mixture of 1 atm. A nitriding procedure is characterized by three parameters: temperature, time and nitriding potential $R_N = \ln [p(NH_3)/p(H_2)^{3/2}]$, where the pressures of ammonia, $p(NH_3)$, and hydrogen, $p(H_2)$, are in Pascal. If the temperature and the nitriding potential correspond to the α-region of the Fe–N Lehrer phase diagram [8,9] (Fig. 1) we call this process α-nitriding (αN). Alternatively, the nitriding process is called γ′-nitriding (γ′N) and ε-nitriding (εN), when R_N and T are in γ′- and e-regions, respectively. After nitriding the samples can be reduced (rd) to α-Fe by annealing in pure H_2 or by α-nitriding.

The texture and phase composition of the samples were characterized by X-ray diffraction (XRD), using a Philips PW1710 spectrometer for θ–2θ (1D-scans) and a Philips X'Pert MRD system for texture measurements (2D-scans). An accurate determination of phase ratios was obtained by transmission Mössbauer spectroscopy (MS) using a standard constant acceleration spectrometer. For the transmission electron microscopy (TEM) study a conventional TEM (CTEM) JEM 200CX and a high resolution TEM (HRTEM)

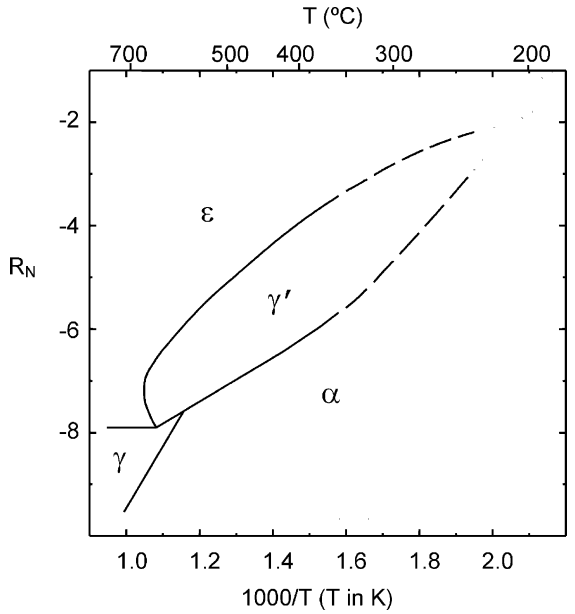

Fig. 1. A revised version of the Lehrer diagram for the Fe–N system [8].

JEOL 4000 EX/II electron microscope were used operating at 200 and 400 kV, respectively. A JEOL 2010F TEM, operated in Circular Scan (CS) mode, was used to perform orientation imaging. The grain size determination was done with several tilting experiments using an ACT: Automated Crystallography for the TEM, from TSL/EDAX and a Gatan dual-view CCD camera (resolution 1000*x*1000 pixels). Grains on top of each other may cause the ACT to measure an incorrect grain size and a different orientation distribution.

Before examination in the TEM, the samples were thinned by two-beam ion milling until perforation.

3. Results

3.1. As-rolled material

Light microscopy and XRD measurements showed that the bulk materials were composed of randomly-oriented micrometer-sized grains. Detailed Mössbauer analysis of the rolled foils [10] shows that, prior to any thermal treatment, the Ti, Cr and Ni atoms are in random solid solution in the iron matrix. The presence of these substitutional atoms produces small lattice dilations, visible as a shift of the XRD lines. The usual XRD θ–2θ scans reveal a strong (1 0 0) texture in as-rolled films, as shown in Fig. 2a for a Fe–Ni–Ti sample. Sometimes (2 2 2) or (2 1 1) diffraction lines are also present. Details of the texture in as-rolled Fe–Ni–Ti films are depicted in Fig. 2b and c, where 2D φ–ψ scans are shown.

Here ψ is the tilt of the sample normal out of the X-ray source-detector scattering plane (offset), and f is the azimuthal angle of the sample rotation around its normal. In Fig. 2b, four peaks corresponding to {2 2 2} planes with a

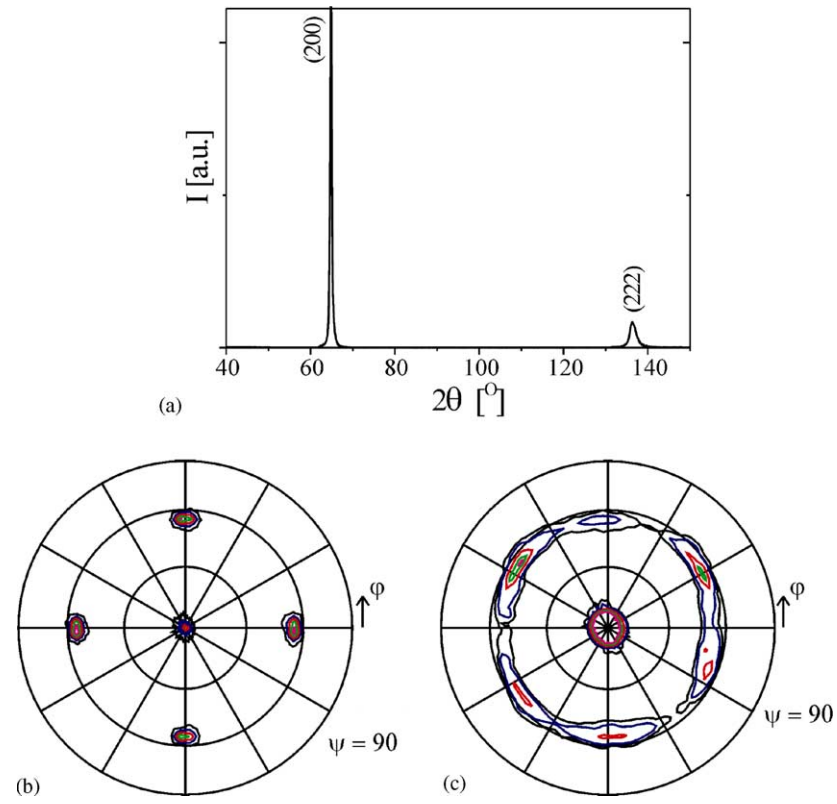

Fig. 2. (a) XRD pattern, (b) pole figure of the {2 2 2} reflection and (c) pole figure of the {2 0 0} reflection for the Fe–Ni–Ti as-rolled material.

common [0 0 1] zone axis normal to the surface are visible. The central peak is the reflection from (2 2 2) planes parallel to the surface. Similarly, in Fig. 2c six {2 0 0} peaks belonging to a [1 1 1] zone axis and a central peak due to (0 0 2) planes parallel to the surface can be seen. From the position of the maxima in the intensity in Fig. 2b and c, it is inferred that the majority of the grains in the as-rolled foils have the (0 0 1) plane parallel to the surface and the [1 1 0] axis in the rolling direction. A smaller fraction of the grains has the (1 1 1) plane parallel to the surface and have [1 1 2] or [1 2 1] axes in the rolling direction. Similar observations were made for as-rolled foils of Fe–Ni–Cr.

In accordance with the XRD results, the TEM diffraction patterns (DP) show the same preference of (1 0 0) planar texture (insert in Fig. 3). The dark field (DF) contrast reveals large areas (around micrometer size) containing bright regions with a size of about 10–20 nm, as shown in Fig. 3. These regions, which represent the strongly defected microstructure of the as-rolled foils, are coherently aligned over large areas, resulting in the overall (1 0 0) texture.

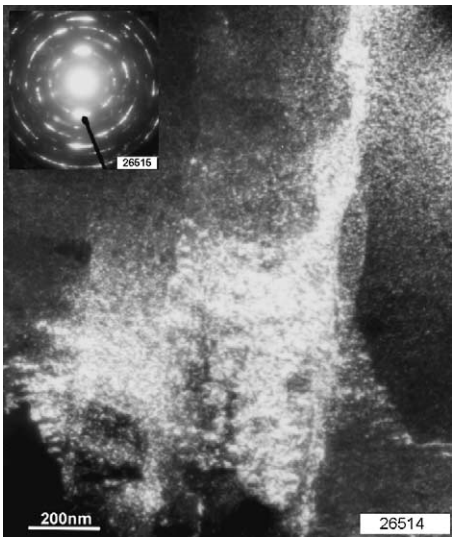

Fig. 3. DF image for the as-rolled Fe–Ni–Ti sample in a {1 0 0}-spot, showing deformation band structure due to rolling.

3.2. $\alpha \leftrightarrow \gamma'$ cycling

The XRD spectra in Fig. 4a and b correspond to a rolled FeTiNi foil first γ'-nitrided (400 °C, 4 h, $R_N = -4.5$) and after a subsequent reduction treatment (400 °C, 4 h, H_2), respectively. In Fig. 4c and d the XRD spectra of an α-prenitrided (300 °C, 20 h, $R_N = -5$) FeTiNi foil after the same γ'N and, respectively, rd treatment are presented. In both cases the intensity of the γ'-(2 0 0) reflection is much larger than the γ'-(2 2 0) reflection intensity indicating that the γ'-phase grows textured with the (1 0 0) planes nearly parallel to the sample surface. The rate of the $\alpha \rightarrow \gamma'$ transformation is reduced by the prenitriding treatment as it is visible from a comparison of Fig. 4a and c. The distribution of the intensity around the γ'-(2 0 0) reflection is complicated but in MS spectra only components corresponding to γ'- or α-phases were found. Therefore this diffraction effect is attributed to a strongly distorted γ'-phase due to stresses built-up during phase transitions. From MS analysis the quantity of γ' formed in both cases were found to be 95 and 50%, respectively. These values are comparable with the estimation of the phase ratio from XRD spectra, indicating that the offset between the α and γ' phases found for the epitaxial Fe films [7] does not play an important role in

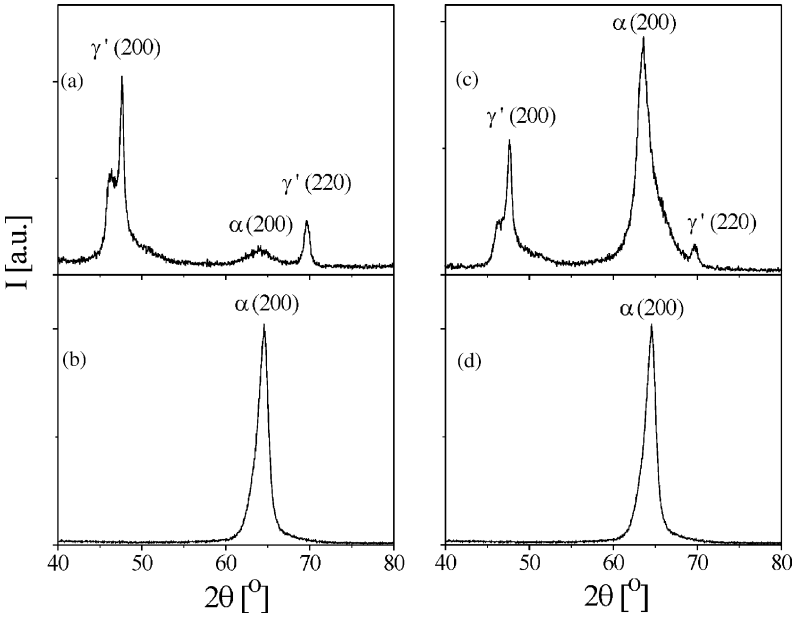

Fig. 4. XRD spectra for Fe–Ni–Ti foils (a) as-rolled and γ'N, (b) as-rolled plus γ'N + rd, (c) αN + γ'N and (d) γ'N + αN + rd.

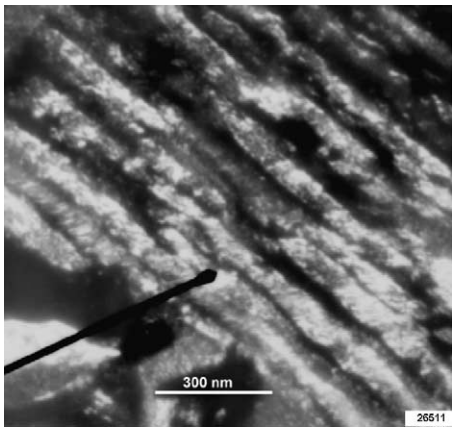

Fig. 5. TEM image, showing lamellae structure for the Fe–Ni–Ti sample after five $\alpha \leftrightarrow \gamma'$ transitions.

the rolled foils. Irrespective of the presence or absence of a pretreatment, the reduction of the foils containing γ'-phase leads practically to the same result, i.e. the reduced samples (Fig. 4b and d) have the same (1 0 0) texture. The distribution of the intensity of the α-(2 0 0) XRD reflection is similar in both reduced samples but it differs from either the as-rolled, or the prenitrided case (see Fig. 2a). The extra broadening of these lines, as compared to the as-rolled situation, for example, can be attributed to an increase of the microstrain rather than to a reduction of the grain size.

In Fig. 5, a dark field image is shown for a Fe–Ni–Ti sample which was first α-nitrided (300 °C, 20 h, $R_N = -5.0$) and then five times cycled through $\alpha \leftrightarrow \gamma'$-phases (380 °C, 4 h, $R_N = -4.5$ for γ' and 380 °C, 4 h, $R_N = -7.5$ for α). The image reveals a structure with long lamellae, with some of the lamellae longer than 1 μm. The corresponding XRD spectrum (not shown here) confirms that, in spite of a final α-nitriding, γ' was the predominating phase after cycling using equal time per step. This observation illustrates the fact that the rate of nitriding or reduction is decreasing with the number of cycles.

Contrary to what was observed for $\alpha \leftrightarrow \gamma'$ cycling of Fe–Ni–Ti samples, for Fe–Cr–Ni foils a relatively small reduction of the texture was observed after $\alpha \leftrightarrow \gamma'$ transformations (Fig. 6). Fig. 6a shows that after four times ($\alpha \leftrightarrow \gamma'$) cycling (380 °C, 3 h, $R_N = -4.5$ for γ' and 380 °C, 3 h, H_2 for a), a small quantity of new α-Fe grains are formed, oriented with the (1 1 0) planes parallel to the surface. In addition, from the 2D scans shown in Fig. 6b, it is evident that the in-plane orientation of crystallites with the [0 0 1] axis normal to the surface becomes distributed over an angular range larger than in the as-rolled foils (see Fig. 2b for comparison). However, the overall texture does not change much, even after cycling several times between the α- and γ'-phases. The fraction of grains with orientation other than (1 0 0) parallel to the surface remains small.

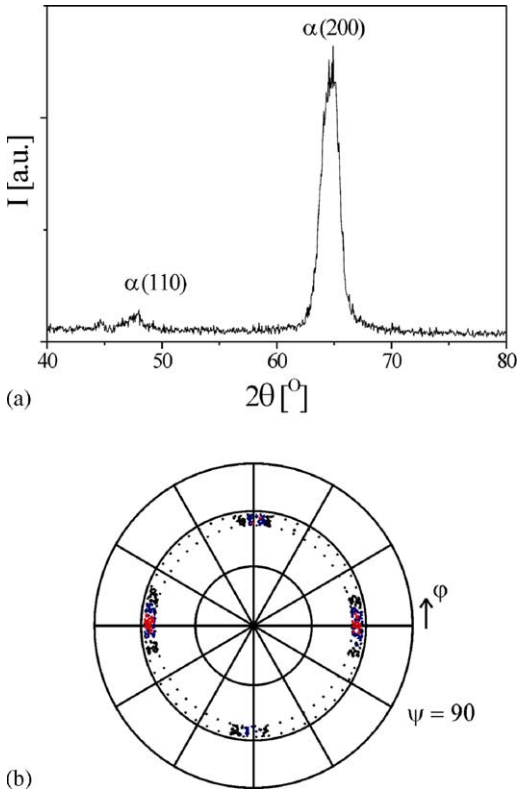

Fig. 6. (a) XRD diffraction pattern for a Fe–Ni–Cr foil cycled four times $\alpha \leftrightarrow \gamma'$; (b) the corresponding pole figure of the {2 2 2} reflections.

3.3. $\alpha \leftrightarrow \varepsilon$ cycling

In Fig. 7a XRD spectra for Fe, Fe–Ni–Ti and Fe–Ni–Cr rolled foils after an ε-nitriding treatment (400 °C, 1 h, NH_3) are presented. After this treatment the Fe foil was completely transformed into the ε-phase. In the Fe–Ni–Cr sample the ε-phase is predominant but γ'-(2 0 0) and (2 2 0) reflections are also visible. After nitriding the Fe–Ni–Ti sample is composed of a mixture of distorted γ'- and ε-phases. The XRD spectra of the ε-nitrided samples after a subsequent reduction treatment (400 °C, 1 h, H_2) are shown in Fig 7b. While the texture of the Fe–Ni–Ti alloy was not changed, in the Fe and Fe–Ni–Cr samples grains with new orientations appear. The most significant reduction of the texture was obtained in the Cr containing sample. Texture measurements (not shown here) indicate that in this latter case the ε-phase grows textured but, after reduction, as expected, a grains with new orientations are formed. The strong broadening, visible in the spectrum corresponding to the Ti containing sample after reduction, is probably due to microstrain built-up during $\alpha \leftrightarrow \gamma'$ and $\alpha \leftrightarrow \varepsilon$ transformations rather than to a reduction in the grain size.

By increasing the number of $\alpha \leftrightarrow \varepsilon$ cycles (ε 400 °C, 1 h, NH_3; α 400 °C, 1 h, H_2) the weakening of the (1 0 0) texture in the Fe–Ni–Cr samples continues (Fig. 8). After the first cycle the (2 0 0) intensity decreases by a factor of 10. After the 7th cycle it has reduced with a factor of 15. The intensity

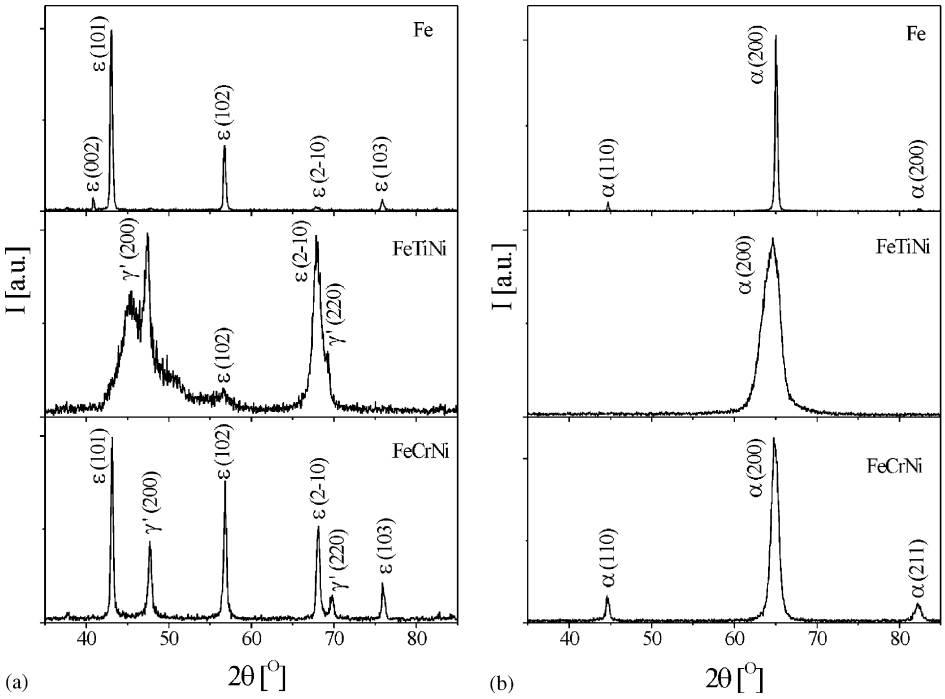

Fig. 7. (a) XRD patterns for Fe, Fe–Ni–Ti and Fe–Ni–Cr foils after εN; (b) the same foils after εN + rd.

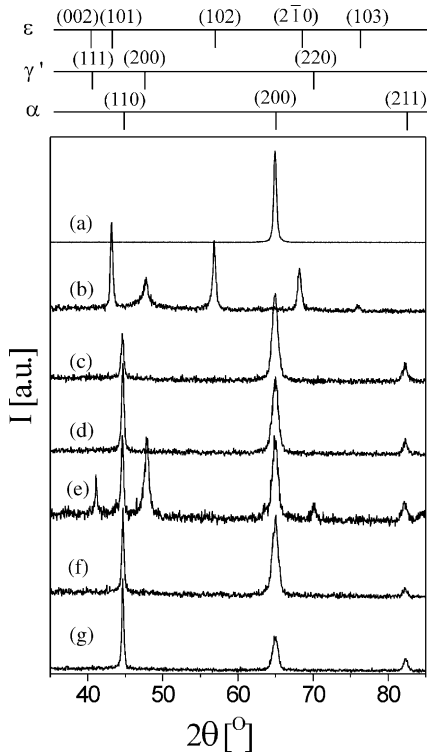

Fig. 8. XRD spectra for a Fe–Ni–Cr foil at different stages of α ↔ ε repeated cycles: (a) as-rolled material, (b) ε-nitrided (1h), (c)–(d) after one and respectively, five α ↔ ε cycles (1h/step), (e) after five cycles and ε-nitrided (1h/step), (f)–(g) after six and respectively, seven α ↔ ε cycles (2–3 h/step). The bar diagrams indicates the peak positions as observed for: (I) α-Fe, (II) γ′-Fe4N and (III) ε-FexN.

of the new (1 1 0) and (2 1 1) reflections, appearing after the first α ↔ ε cycle (Fig. 8c), increases continuously with the number of transformations (see Fig. 8c,d) while the intensity of the (2 0 0) reflection decreases. After five cycles and an additional ε-nitriding treatment the sample was transformed into a mixture of α- and γ′-phases (Fig. 8e). In order to obtain a complete e transformation it was necessary to increase the nitriding time from 1 h to 2 h. This illustrates the fact that similarly to the α ↔ γ′ phase transitions the velocity of the α ↔ ε phase transitions decreases with increasing

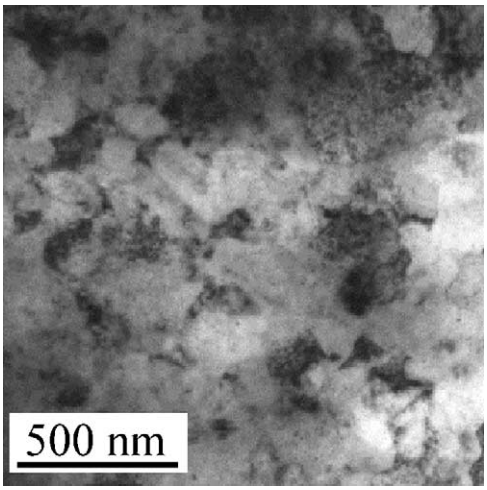

Fig. 9. A TEM BF image of the microstructure of the 5 × (α ↔ ε) cycled Fe–Ni–Cr sample.

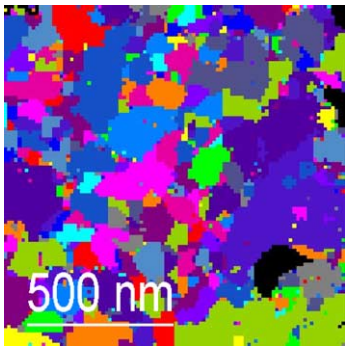

Fig. 10. The grain map of the of the $5\times(\alpha \leftrightarrow \varepsilon)$ cycled Fe–Ni–Cr sample.

number of cycles. The time per step for the next cycles was progressively increased (up to 3 h for the 7th cycle) in order to have a complete ε transformation.

The TEM DF image presented in Fig. 9 shows the complex structure of the sample after five cycles. The new grains formed have a reduced density of defects as is suggested by a much weaker variation of the contrast inside the grains as compared to the as-rolled case. The grain refinement effect is evident from the grain map image presented in Fig. 10. The majority of the grains after five cycles has an in-plane average size of the order of 100–200 nm. However, when the number of cycles was further increased the grain structure started to coarsen again.

An important reduction of the texture was obtained for a Fe–Ni–Ti prenitrided sample after an $\alpha \leftrightarrow \varepsilon$ cycle at 500 °C (Fig. 11), contrary to the lower temperature case (400 °C, Fig. 4b and d).

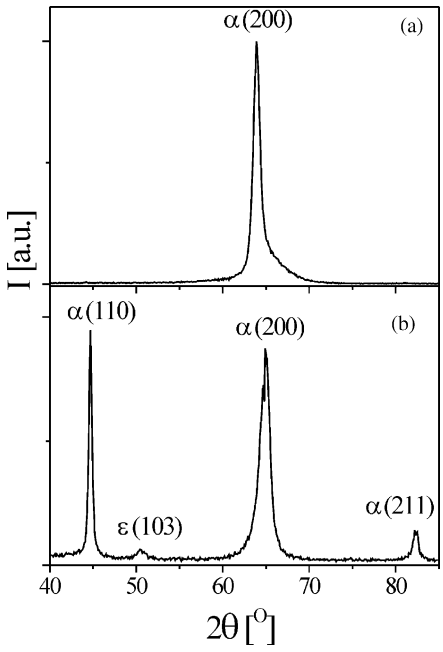

Fig. 11. (a) XRD pattern after αN and (b) after $\alpha N + (\alpha \leftrightarrow \varepsilon)$ at 500 °C for a Fe–Ni–Ti sample.

4. Discussion

4.1. Kinetic effects

In addition to the formation of precipitates α-nitriding leads to a certain structural recovery. This effect has been observed by the authors in the TEM [10] and it is also confirmed by Positron Annihilation (PA) measurements [11]. Assuming that the kinetic barriers for the phase transitions are reduced by the presence of defects, the observed retardation in the $\alpha \rightarrow \gamma'$ transition after an α-nitriding pre-treatment may be explained by such a partial recovery phenomenon. The formation of TiN precipitates may also influence the kinetics of the $\alpha \rightarrow \gamma'$ transformation.

When a new phase nucleates and grows coherently with the parent phase, the defects, which have not been annealed at that moment, will either partially annihilate or partially transform into new defects. New defects are created but to a smaller extent [11]. The overall decrease of the rolling-induced defects during nitriding and reduction results in a slowing down of the transformation velocity with every round of the cycling (Fig. 8). In this case the new phase grows, on average, more slowly after each step and a longer period is required in order to complete the transformation.

4.2. $\alpha \leftrightarrow \gamma'$ cycling of Fe–Ni–Ti

The formation of the γ'-phase in γ'-nitrided Fe–Ni–Ti or Fe–Ni–Cr foils is a typical bcc $\rightarrow$ fcc transformation described, roughly, by the Bain OR. As argued in the introduction, the result after a bcc $\leftrightarrow$ fcc reversible transformation with all possible channels should be the appearance of bcc grains with new orientations like with (1 1 0) or (2 2 1) planes parallel to the sample surface. Intermediate fcc grains should also be formed with the (1 0 0) or (1 1 0) planes parallel to the surface. In the case of the Ti containing material the γ'-phase was formed with a (100) predominant texture and in the reverse transformation the final α-phase does not show other orientations than the original (1 0 0). These effects are attributed to the TiN precipitates as it will be explained in the next section.

Because the time used for the γ'-nitriding, 4 h, is longer than the time required for formation of TiN precipitates (2 h) and, because the rate determining the γ'-phase formation is given by the intake of nitrogen, it is expected that in the as-rolled and γ'-nitrided foil the TiN precipitates are formed first. In both cases the TiN precipitates are formed parallel with the {1 0 0} bcc matrix planes. They form a network that is stable against further ripening at temperatures below 500 °C. This network increases the strength of the material. In this way the stress release in the plane of the foil by creation of dislocations becomes more difficult preventing the formation of the γ'-phase with (1 1 0) planes parallel to the surface. During the back transformation a similar argumentation holds. This explains why (1 1 0) bcc planes parallel to

the surface are not formed, so that the material has practically the same texture as observed before cycling (Fig. 4b and d). The complicated distribution of the diffracted intensity on both sides of the γ′-(2 0 0) peak (Fig. 4a and c) can be explained by the presence of strain. In addition, the presence of the TiN precipitates in the γ′-phase can lead to a similar lattice dilation and excess nitrogen as observed in the α-nitrided bcc-phase [10].

4.3. α ↔ γ′ cycling of Fe–Ni–Cr

The CrN precipitates are less stable than the TiN precipitates [10]. At 400 °C, as the time of the applied treatment increases, the CrN precipitates form, dissolve and coarsen at grain boundaries. Therefore it is expected that as the number of cycles increases the phase transformations and the evolution of the precipitates take place simultaneously. Consequently, the CrN will influence less the phase transformations than the TiN precipitates. In the Fe–Ni–Cr material the γ′-phase forms with (1 0 0) and (1 1 0) planes parallel to the sample surface. If the three possible channels (one perpendicular and two in the plane of the foil) would be realized with equal probability, the intensity of the (2 2 0) and the (2 0 0) reflections would be about equal. The ratio of the two intensities in the γ′-nitrided foil was 0.5, smaller than expected, indicating that the α → γ′ transformation takes place with a similar preference for a (1 0 0) textured γ′-phase. Thus, even in a sample with less influence of precipitates the release of stress perpendicular to the surface is preferred. This explains why during the reduction treatment only a small fraction of a grains with other orientation than found initially are formed. In addition, after four α ↔ γ′ cycles, the (2 0 0) reflection in the Cr containing material broadens and the spread of the diffracted intensity in 2D-XRD scans increases in the φ direction (Fig. 6b). At least two effects can lead to such broadening and spread: the increase of the strain in the material and/or the increase of the misalignment between the α- and γ′-phases. Both effects are results of the bcc → fcc transformations.

4.4. α ↔ ε cycling of Fe–Ni–Ti

The α → ε transformation of pure Fe occurs at 300 °C via the intermediate γ′-phase [7]. For Ti and Cr containing alloys ε-nitrided at 400 °C, mixtures of ε- and γ′-phases were obtained. This is an indication that in the rolled foils the formation of the hcp ε-phase takes place via an fcc → hcp transformation. In such a transformation the {1 1 1} fcc planes become {0 0 0 1} hcp planes but of course the stacking sequence is different. The correct stacking sequence can be obtained if shearing in the [1 1 $\bar{2}$] direction takes place on every other (1 1 1) fcc plane. It is evident that such a transition requires atomic reshuffling. When TiN precipitates are present in the material they hinder this reshuffling of the Fe atoms, stabilizing in this way the γ′-phase. This effect is visible in Fig. 7a, where the Ti containing alloy consists of a mixture of ε- and γ′-phases, while the Fe or Fe–Ni–Cr materials are almost completely transformed under the same nitriding conditions. After reduction the Fe–Ni–Ti alloy presents the same initial {1 0 0} texture. This implies that the orientation of the TiN precipitates did not change during the α ↔ ε transitions and they act as anchors for the initial texture.

At 500 °C the TiN precipitates formed are much bigger and the coherency is partially lost. At this temperature the diffusion of Ti and Fe atoms becomes significant and helps the strain relief required for phase transformations and probably leads to a change of the orientation of the precipitates. The anchoring effect of TiN precipitates is lost and, as argued in the introduction, during the complex α ↔ ε transitions grains with new orientations are formed (Fig. 11).

4.5. α ↔ ε cycling of Fe–Ni–Cr

For the Cr containing material, α ↔ ε cycled at 400 °C, the e-phase grows with a few crystalline orientations (Fig. 7), i. e. with the (1 0 1), (1 0 2), (2 $\bar{1}$ 0), (1 0 3) planes parallel to the surface. However, 2D XRD scans (not shown here) reveal that the in-plane orientation of the ε crystallites is not at random. In contrast with this observation, the new α grains formed in the back transition do not show a preferred in-plane orientation. This may be due to the large number of possible channels for the back transformation, in addition to strain effects. Furthermore, 2D-scans of foils after repeated phase transitions showed that only the grains that are transformed back into the initial state, i.e. those with the (1 0 0) planes parallel to the surface, present an in-plane preferred orientation. Increasing the number of cycles leads to a decrease of the intensity of the (200) reflection of the α-phase (Fig. 8). The conclusion is that in the Cr containing alloy, the α ↔ ε cycling produces a grain reorientation. The effect of one cycle on the texture reduction on the Fe–Ni–Cr foil was found to be more important than for the pure Fe (Fig. 7). This can be attributed to the change in orientation of the CrN precipitates during the time that the sample is at high temperature. This may increase the difference in channels that are active during formation and reduction of the ε-phase.

Light microscopy observations show that the average grain size in the as-rolled or α-nitrided material is in the micrometer range. A clear reduction of the grain size was obtained for the Fe–Ni–Cr material after five α ↔ ε cycles (Figs. 9 and 10). The repeated phase transformations have produced grains with smaller dimensions in both longitudinal and transversal directions. Increasing the number of cycles even further did not produce additional grain refinement. On the contrary, the structure became coarser after 15 cycles. It appears that the competition between the formation of new grains by phase transformation and grain growth due to annealing results in a minimum grain size of about 100 nm obtained after five cycles.

5. Conclusions

In summary: phase transformations during gaseous nitriding in Fe–Ni–Ti and Fe–Ni–Cr cold rolled foils were studied. Severe deformation caused by cold rolling leads to formation of a large density of nucleation sites for new phases (i.e. γ' and ε) and reduced kinetic barriers for the phase transformation. The resulting fast growth of a new phase is found to be retarded at every new cycle of $\alpha \leftrightarrow \gamma'$ or $\alpha \leftrightarrow \varepsilon$ transformations. This effect is interpreted as an increase of the kinetic barrier for the phase transformation due to annihilation of rolled-induced defects during cycling.

The $\alpha \leftrightarrow \gamma'$ transformation do not produce significant grain reorientation in both Cr and Ti containing alloys. For the Cr containing alloy this is explained by the preferential way of releasing the stresses, perpendicular to the plane of the foils, during phase transformation. For the Ti containing alloy the similar effect is amplified by the presence of the stable network of TiN precipitates which strengthens the alloy and makes the accommodation of stresses in the plane of the foil even more difficult. Therefore, at low temperatures ($\leq$400 °C) the coherent TiN precipitates can be regarded as anchors of the initial texture, i.e. during an $\alpha \leftrightarrow \gamma'$ martensitic phase transformation the formation of grains with new orientations is prevented. The same TiN precipitates retard the formation of the ε-phase in an $\alpha \leftrightarrow \varepsilon$ transformation at 400 °C, stabilizing the γ'-phase and preventing the change of the texture. At 500 °C, the diffusion of Ti and Fe atoms becomes significant and helps the relief of strain as required for phase transformations and leads probably to a reorientation of precipitates. Consequently, the diffusion diminishes the anchoring effect of precipitates leading to an important reduction of the texture.

Grain refinement and grain reorientation take place after $\alpha \leftrightarrow \varepsilon$ transformations in Fe–Ni–Cr alloy at 400 °C. The presence of the continuously transforming CrN precipitates contributes to the reduction of texture, which was found to be more important in this material than in pure Fe. By increasing the number of cycles a progressive reduction of the texture was obtained. The starting material possesses grains in the micrometer range. After five cycles the grain size is of the order of 100 nm. A further increase of the number of cycles leads to grain coarsening.

The materials obtained by cold rolling and repeated phase transformations did not show soft magnetic properties [12]. The new grains have random orientations but their average grain size is still larger than the critical size imposed by the random anisotropy model [13] and then the effective magnetocrystalline anisotropy is still large. The method can be successfully used for obtaining ultra-fine-grained structures in a surface layer of a few micrometers. Such a surface layer can exhibit interesting mechanical properties like an increased hardness or improvement of the fracture resistance.

References

[1] F.J. Humphreys, P.B. Prangnell, R. Priester, Current Opinion in Sol. Stat. Mat. Sci 5 (2001) 15.
[2] E. Arzt, Acta Mater. 46 (1998) 5611.
[3] A.H. Chokshi, A. Rosen, J. Karch, H. Gleiter, Script. Metall. 23 (1989) 1679.
[4] G. Herzer, IEEE Trans. Magn. 26 (1990) 1397.
[5] A.K. Ibraheem, R. Priestner, J.R. Bowen, P.B. Prangnell, F.J. Humphreys, Iron Steelmak. 28 (2001) 203.
[6] V.V. Sagaradze, I.G. Kabanova, Mat. Sci. Eng. A 273–275 (1999) 457.
[7] A.V. Mijiritskii, D.O. Boerma, Phys. Rev. B 64 (2001) 1.
[8] E.H. du Marchie van Voorthuysen, B. Feddes, N.G. Chechenin, D.K. Inia, A.M. Vredenberg, D.O. Boerma, Phys. Stat. Sol. (a) 177 (2000) 127.
[9] E. Lehrer, Z. Electrochemie 30 (1930) 383.
[10] N.G. Chechenin, A. Chezan, C.B. Craus, D.O. Boerma, P.M. Bronsveld, J.Th.M. De Hosson, L. Niesen, Metall. Mater. Trans. 33A (2002) 3075.
[11] N.G. Chechenin, A. Van Veen, R. Escobar Galindo, H. Schut, A. Chezan, D.O. Boerma, J. Phys.: Condens. Matter 13 (2001) 5937.
[12] C.B. Craus, A.R. Chezan, D.O. Boerma, L. Niesen, J. Magn. Magn. Mat 263 (2003) 47.
[13] G. Herzer, IEEE Trans. Magn. 26 (1990) 1397.